Revista Internacional de Métodos Numéricos para Cálculo y Diseño en Ingeniería

Tech Science Press

https://doi.org/10.32604/rimni.2026.086620

ARTICLE

Optimization of Layout and Hub Height for Offshore Wind Farm with an Advanced Wake Analytical Model

Lihua Mi[1], Xin Zhang[1], Fei Zhang[2], Hui Chen[1], Pinhan Zhou[3] and Qinghui Lai[1,*]

[1]College of Architecture and Energy Engineering, Wenzhou University of Technology, Wenzhou, China
[2]Power China Guiyang Engineering Corporation Limited, Guiyang, China
[3]College of Civil and Environmental Engineering, Changsha University of Science and Technology, Changsha, China

*Corresponding Author: Qinghui Lai. Email: 20240119@wzut.edu.cn

Received: 02 June 2026; Accepted: 31 July 2026; Published: 06 November 2026

ABSTRACT: Wake interactions among wind turbines strongly influence wind farm power generation and economic performance, making wind farm layout optimization (WFLO) essential for efficient energy harvesting. This study develops an integrated optimization framework by coupling a previously validated three-dimensional elliptic super-Gaussian wake model (3DESG) with a genetic algorithm (GA). The contribution of the present work is the optimization coupling, implementation, and controlled comparison of baseline, hub-height-only, layout-only, and simultaneous layout-height optimization scenarios under a prescribed southwesterly inflow (225° in meteorological convention; 45° downstream heading). The 3DESG formulation is adopted from earlier work without recalibration, while the GA searches turbine coordinates and, where applicable, discrete hub-height assignments. Increasing the aligned baseline hub height from 50 to 80 m increases total power from 4759.91 to 5594.37 kW, whereas layout optimization at 80 m increases total power to 8285.81 kW. This corresponds to a 48.11% increase relative to the 80 m aligned baseline and a 74.07% increase relative to the 50 m aligned baseline. The cost-per-normalized-power indicator decreases from 1.20 for the 80 m aligned baseline to 0.81 for the optimized layout. Simultaneous layout-height optimization produces a similar solution because the optimal hub-height selection converges to 80 m for all turbines in the present two-height design space. These findings indicate that turbine placement has a stronger effect than hub-height adjustment in this controlled single-direction case; however, this conclusion is restricted to a fixed turbine number, two discrete hub heights, a single best GA run, and a simplified economic model.

KEYWORDS: Offshore wind farm; wake analytical model; genetic algorithm; layout and hub height optimization; prevailing wind direction

1 Introduction

The global transition toward low-carbon energy systems has intensified interest in wind energy as a major renewable electricity source [1,2]. Wind-farm performance and economic viability are strongly affected by wake interactions and farm configuration. Consequently, wind farm layout optimization (WFLO) has become a central design problem for increasing energy production while controlling project cost [3–5].

Computational fluid dynamics (CFD) is widely used to investigate wind-turbine aerodynamics, atmospheric-flow effects, and wake development. Ma et al. [6] analyzed coupled aeroelastic wake behavior, Li et al. [7] examined the effects of ground roughness and atmospheric stratification using large-eddy simulation, and Cai et al. [8] investigated yawed inflow and blade-tower interaction. High-fidelity wake simulations have also been reported for individual turbines and large wind farms [9–11]. Although these

Copyright © 2027 The Authors. Published by Tech Science Press. This work is licensed under a Creative Commons Attribution 4.0 International License, which permits unrestricted use, distribution, and reproduction in any medium, provided the original work is properly cited.

approaches provide detailed flow information, their computational cost can be restrictive in WFLO, where many candidate configurations must be evaluated. Analytical wake models therefore remain useful for optimization-oriented engineering studies.

Hub-height and three-dimensional wind-farm design have been investigated using several optimization objectives. Lee et al. [12] showed that the hub height maximizing annual net profit depends on wind conditions. Vasel-Be-Hagh and Archer [13], Abdulrahman and Wood [14], and Chen et al. [15] further demonstrated that hub-height selection can alter the trade-off between energy production and cost. These studies provide the appropriate support for the hub-height discussion in the present manuscript.

Considerable effort has also been devoted to turbine-position optimization. Yang et al. [16] developed a modified genetic algorithm for WFLO, Liu et al. [17] incorporated offshore engineering cost and seabed constraints, and Bai et al. [18] proposed an adaptive evolutionary framework. Wake-model-based layout studies [19], simultaneous layout and hub-height optimization [20], and three-dimensional turbine positioning [21] have further demonstrated the importance of horizontal and vertical design variables. In addition, uncertainty in wind conditions has been treated explicitly in layout-optimization studies [22,23].

Although significant progress has been achieved, comparatively few studies have used the same wake model, turbine number, domain, inflow direction, and economic indicator to isolate the relative effects of hub-height-only, layout-only, and simultaneous layout-height optimization. Because horizontal and vertical turbine spacing influence different components of wake overlap, a controlled comparison is useful for identifying which design variable drives the performance differences under a prescribed inflow condition.

To address this need, the present study couples a previously validated 3DESG wake model with a GA optimizer and evaluates four controlled scenarios: fixed aligned baselines, hub-height-only optimization, layout-only optimization, and simultaneous layout-height optimization. The cost-per-normalized-power indicator is used to compare power production with the simplified hub-height-dependent cost proxy. The analysis is intentionally restricted to a southwesterly inflow (225° in meteorological convention; 45° downstream heading) so that the effects of the design variables can be compared under the same inflow condition.

The 3DESG wake model itself is not newly derived in this manuscript; it is the aerodynamic evaluation module adopted from the authors' previous work [24]. The present contribution consists of: (i) a reproducible 3DESG-GA coupling procedure for wind-farm optimization, (ii) a controlled case matrix that separates hub-height-only, layout-only, and simultaneous layout-height optimization, and (iii) a quantitative comparison of power, wake-loss mitigation, and cost-per-normalized-power indicators under the same turbine number and wind direction. This attribution is used consistently throughout the manuscript.

The remainder of this paper is organized as follows. Section 2 introduces the wake model and genetic algorithm framework employed in the optimization procedure. Section 3 presents and discusses the optimization results under different scenarios, and Section 4 summarizes the principal findings and conclusions.

2 Methodologies

To characterize aerodynamic interactions among wind turbines, the present study employs the three-dimensional elliptic super-Gaussian wake model (3DESG) established and validated in the authors' earlier work [24]. In this manuscript, the 3DESG model is used as a fixed wake-evaluation component. The new work (shown in Fig. 1) lies in coupling this component with a GA optimizer, defining the design variables and constraints, and comparing the C1-C4 optimization scenarios. No wake-model coefficient is recalibrated for the present optimization cases.

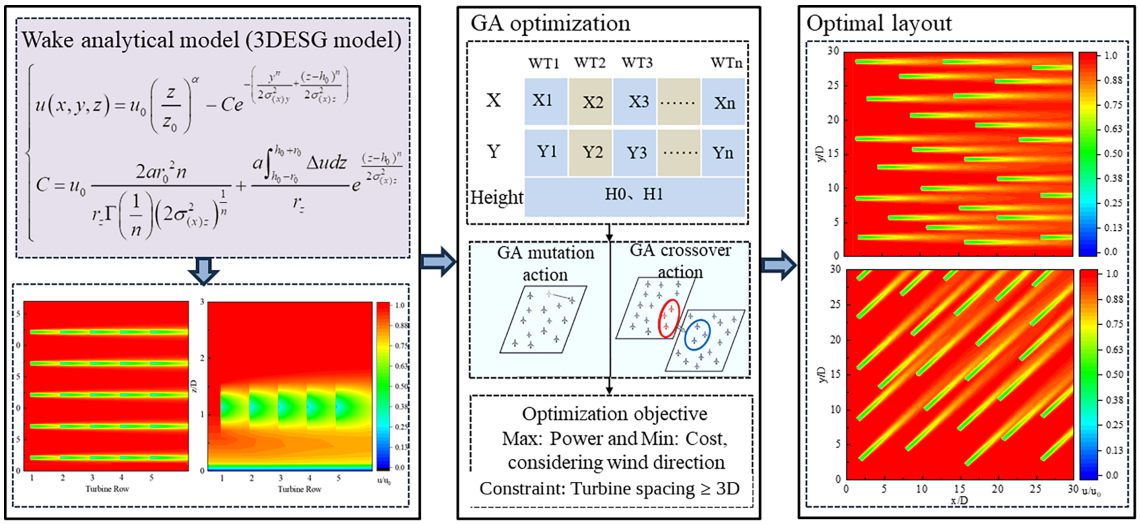


Figure 1: Flowchart of the proposed method for WFLO.

2.1 3DESG Wake Model

This section summarizes the 3DESG formulation established in the authors' previous study [24], which provides the theoretical basis for the present analysis. The detailed derivation and validation are reported in [24], where the model was compared with representative wake data and benchmark formulations. Accordingly, the results below should be interpreted as the performance of the optimization framework when driven by the previously validated 3DESG wake predictor, rather than as a new validation of the wake model.

The wake-induced velocity reduction, denoted by ΔV, is expressed as:

$$\Delta V = \left(u_0 \frac{2a{r_0}^2 n}{r_z \Gamma\left(\frac{1}{n}\right)\left(2\sigma_z^2\right)^{\frac{1}{n}}} + \frac{a\int_{h_0-r_0}^{h_0+r_0} \Delta u dz}{r_z} e^{\frac{(z-h_0)^n}{2\sigma_z^2}} \right) e^{-\left(\frac{y^n}{2\sigma_y^2}+\frac{(z-h_0)^n}{2\sigma_z^2}\right)} \tag{1}$$

where u_0 and r_0 denote the wake velocity at hub level and the rotor radius, respectively. h_0 corresponds to the hub height. Γ represents the gamma function. The angle brackets in Eq. (1) are grouping symbols only and do not denote an average, expectation, or inner product; a is the dimensionless wake-deficit amplitude coefficient in the 3DESG formulation. r_z defines the wake radius in the vertical direction. σ_y and σ_z characterize the wake width along the lateral and vertical coordinates, respectively. The vertical wake radius is determined as $r_z = k_z x + r_0 = 2.81\sigma_z$. k_z denotes the vertical wake expansion coefficient and is evaluated using Eq. (2).

$$k_z = 0.2433 C_T^{0.4297} I_0^{0.4707} \tag{2}$$

where C_T represents the thrust coefficient, and I0 is the inflow turbulence intensity. The wake-expansion and super-Gaussian formulations follow the analytical modeling approaches described in [25,26]. The parameter n is obtained from an exponential relationship, while Δu quantifies the hub-level wake deviation induced by wind shear. These variables are defined as follows:

$$\begin{cases} n = c_1 e^{c_2 x} + 2 \\ \Delta u = u(z) - u_0 = u_0 \left(\dfrac{z}{z_0}\right)^{\alpha} - u_0 \end{cases} \tag{3}$$

where c_1 and c_2 characterize the intrinsic variability associated with wake development. z_0 denotes the reference elevation; α corresponds to the wind shear exponent.

2.2 GA Algorithm

A genetic algorithm (GA) is adopted as the optimizer [16–18]. For position-optimization cases, one chromosome is encoded as an ordered vector of integer grid indices, and the indices are converted to physical turbine coordinates using a grid resolution of 100 m (approximately 1.43D). For height-optimization cases, a discrete height gene is added and mapped to one of the two available hub-height options, 50 or 80 m. The wind farm contains 25 turbines in a 2 km × 2 km domain with rotor diameter D = 70 m. The GA method uses a population size of 100, a maximum generation number of 500, boundary margins of 2D from the domain edges, and the default ranking, selection, crossover, and mutation operators of the adopted scikit-opt GA routine. A hard spacing constraint is imposed by assigning an infeasible fitness penalty when the center-to-center distance between any two turbines is smaller than 3D. The computational procedure of the proposed 3DESG-GA optimization framework is summarized in Algorithm 1.

Algorithm 1: 3DESG-GA fitness evaluation and optimization procedure

Input: turbine number, rotor diameter, search-domain bounds, hub-height set, prevailing wind direction, 3DESG parameters, including free-stream wind speed U∞ and inflow turbulence intensity I0, and GA parameters.

1. Encode each candidate wind farm as turbine coordinates and, for C2/C4, discrete hub-height genes.
2. Convert integer grid genes to physical coordinates using Δg = 100 m (approximately 1.43D); sort turbines in the inflow direction.
3. For each turbine, compute the local inflow speed at its hub height.
4. For each downstream turbine, evaluate upstream wake deficits using the 3DESG model and combine multiple wakes by the root-sum-square rule.
5. Convert effective turbine wind speed to turbine power and sum the farm power.
6. Compute the total cost and the cost-per-normalized-power indicator defined in Eqs. (5) and (6).
7. If any turbine pair violates the minimum spacing constraint, assign the penalty fitness.
8. Apply GA ranking, selection, crossover, and mutation to generate the next population.
9. Stop at the maximum generation number of 500 and output the best chromosome and its power/cost indicators.

2.3 Optimization Targets

The objective of wind farm spatial optimization, encompassing both turbine hub height and layout, is to identify the most favorable coordinates (x, y) and hub elevation (h) for each turbine, which can be expressed mathematically as:

$$\begin{cases} min\, f_X = C_P(x_i, y_i, h_i), \\ s.t. X_L <= x_i <= X_U, Y_L <= y_i <= Y_U, H_L <= h_i <= H_U \\ d_{ij} >= 3D \end{cases} \tag{4}$$

where the objective function, constraint functions, coordinate bounds, hub-height bounds, and inter-turbine spacing constraint are defined in Eq. (4). The design variables are turbine horizontal coordinates and, for C2 and C4, the discrete hub-height assignment. The objective is the minimization of the cost-per-normalized-power indicator defined in Eq. (6). For height optimization, two discrete values are considered, 50 and 80 m. The farm area is 2 km × 2 km, with horizontal bounds from 0 to 2000 m in both coordinate directions. The optimization enforces a minimum center-to-center spacing of 3D by assigning a penalty fitness to infeasible chromosomes.

3 Results of Hub Height and Layout Optimization

3.1 Optimization Target

In this section, the cost-per-normalized-power indicator defined in Eq. (6) is selected as the optimization objective under a southwesterly inflow (225° in meteorological convention; 45° downstream heading). A lower value denotes a lower simplified cost per unit of normalized power. Four scenarios are analyzed: fixed aligned baseline layouts, hub-height-only optimization for the aligned layout, layout-only optimization at a fixed hub height, and simultaneous layout-height optimization. The cost function and optimization objective are given by Eqs. (5) and (6):

$$C_{total} = \sum_{i=1}^{N} kh_i[2/3 + 1/3exp(-0.00174N^2)] \tag{5}$$

$$min\, C_P = C_{total}/\sum_{i=1}^{N} P_i/P_0 \tag{6}$$

In these equations, N represents the fixed number of turbines. Because all C1–C4 cases use the same $N = 25$ turbines, the cost term mainly distinguishes hub-height choices rather than turbine number in the present layout comparison. The coefficient k accounts for the relative cost correction between the two hub-height options. Following [27], the 50 m tower is assigned a lower relative cost than the 80 m tower, and the ratio used in the calculation is $k = 9/11$. Therefore, the economic model should be understood as a simplified cost proxy rather than a full levelized-cost-of-energy model; installation, cabling, operation, maintenance, and seabed-condition costs are not explicitly modeled. Table 1 depicts the definition of variables fixed or optimized in Cases C1–C4.

Table 1: Definition of variables fixed or optimized in cases C1–C4.

Case	Variables Fixed	Variables Optimized	Purpose
C1-50	Aligned 5 × 5 layout; h = 50 m	None	Low-height baseline
C1-80	Aligned 5 × 5 layout; h = 80 m	None	High-height baseline
C2	Aligned 5 × 5 layout; x_i and y_i fixed	Discrete hub height $h_i \in \{50, 80\ m\}$	Height-only optimization
C3	Hub height fixed at 80 m	Turbine coordinates x_i and y_i	Layout-only optimization
C4	Turbine number and domain fixed	Turbine coordinates x_i, y_i and discrete h_i	Coupled layout-height optimization

3.2 Case C1—Aligned Layout at the Same Height

Regardless of whether the objective function is to maximize power output or minimize the cost-per-normalized-power indicator, the positions and hub heights of the turbines in the baseline conditions C1 are fixed and independent of the optimization objectives. Fig. 2 illustrates the normalized wind speed distribution and normalized power output of each turbine at different hub heights (50 and 80 m, in the x-y plane). The following conclusions can be drawn from the figure:

(a) At both heights (50 or 80 m), since the turbine's rotational plane is always aligned with the wind direction, the wind speed in the turbine's wake exhibits a symmetrical distribution along the wind direction angle. As the downstream distance increases (in the direction of the incoming flow), the

interference from the upstream turbine's wake on the downstream turbine intensifies, leading to an increase in both the width and length of the wake loss experienced by the downstream turbine. Additionally, the wake interference demonstrates a superposition effect, resulting in the most severe wake loss for the furthest downstream turbine. Furthermore, as the hub height increases (from 50 to 80 m), the extension length of the wake loss at the hub center decreases, diminishing the superposition effect of the upstream turbine's wake on the downstream turbine, thereby reducing the interference and increasing the power output of the downstream turbine.

(b) As the hub height increases, the power output of each turbine also rises. At both heights, the power output of the turbines exhibits a symmetrical distribution along the flow direction. With increasing downstream distance, the superposition effect of the upstream turbine's wake on the downstream turbine intensifies, causing a gradual decrease in the power output of the downstream turbine, with the rate of decrease gradually diminishing. For example, at a hub height of 80 m, the normalized power outputs of the turbines at the center of the region (in the direction of the incoming flow) are 1, 0.477, 0.436, 0.424, and 0.419, with corresponding reductions of 52.3%, 4.1%, 1.2%, and 0.5%.

(c) Further calculations give cost-per-normalized-power indicator values of 1.16 at 50 m and 1.20 at 80 m. The 50 m aligned baseline has a lower simplified cost indicator, but its total power is 4759.91 kW. The 80 m aligned baseline increases total power to 5594.37 kW, corresponding to normalized total powers of 13.79 and 16.21, respectively, when both are normalized by the 80 m single-turbine reference power.

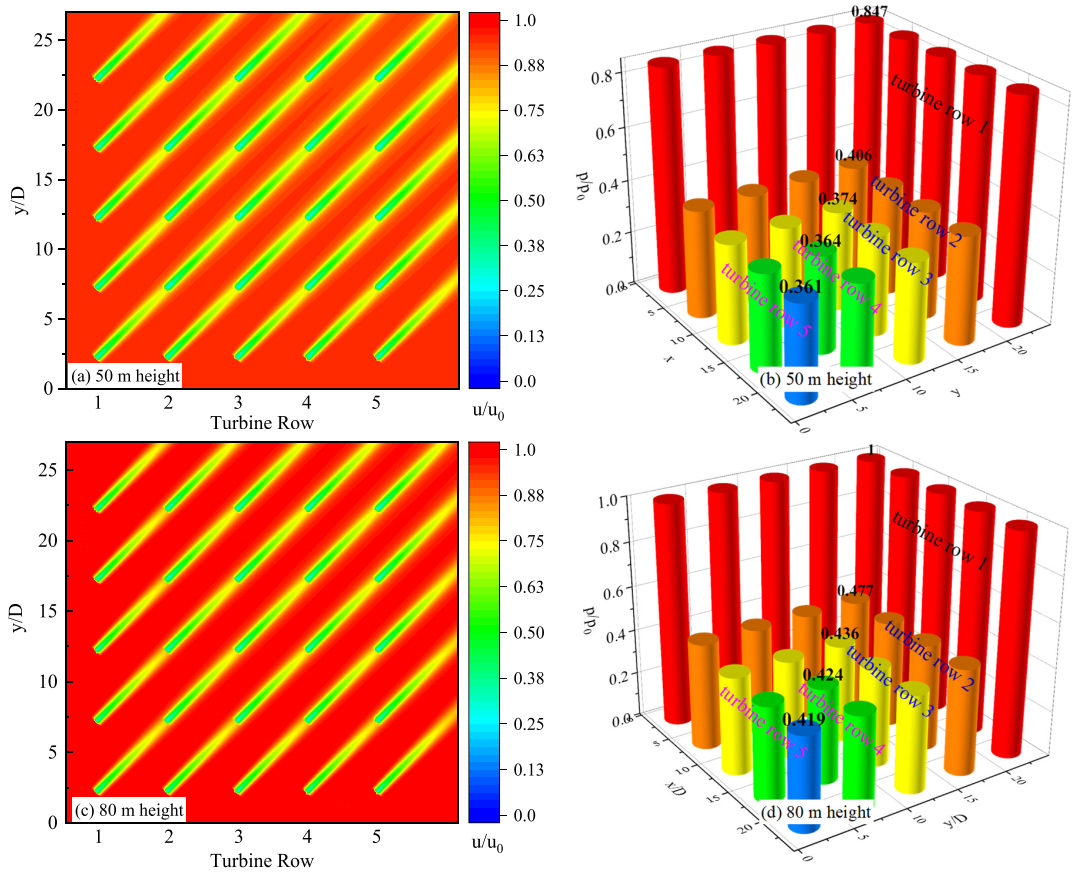


Figure 2: Normalized wind speed distribution and power generation at different heights (50, 80 m).

3.3 Case C2—Hub-Height Optimization for an Aligned Layout

Figs. 3 and 4 illustrate the normalized wind speed distribution and normalized power distribution at different hub heights (50 and 80 m, *x*-*y* cross-section). The key conclusions drawn from the figures are as follows:

(a) After optimization, the hub height of the first row of turbines is uniformly set at 80 m, while the first turbine in each of the remaining four rows (in the flow direction) also has a hub height of 80 m. Additionally, the hub heights of turbines across rows exhibit an alternating distribution, which minimizes the interference of upstream turbine wakes on downstream turbines. Moreover, the number of turbines at a height of 80 m significantly exceeds that of turbines at 50 m, indicating a more rational layout of the wind farm.

(b) The normalized power distribution of each turbine aligns with the normalized wind speed distribution. Specifically, the power output of turbines in each row (in the flow direction) shows a symmetrical trend. Furthermore, in the flow direction, the power output of turbines with a hub height of 80 m is significantly greater than that of turbines with a hub height of 50 m, and the power distribution exhibits an alternating pattern (from high to low).

(c) In comparison with the baseline aligned case C1 at 80 m, C2 changes only the hub-height assignments while keeping the turbine coordinates fixed. Under the aligned layout, hub-height selection reduces the cost-per-normalized-power indicator from 1.20 for C1-80 to 1.01 for C2 and increases total power from 5594.37 to 6066.15 kW. The improvement is beneficial but smaller than that obtained by turbine-position optimization in C3 and C4.

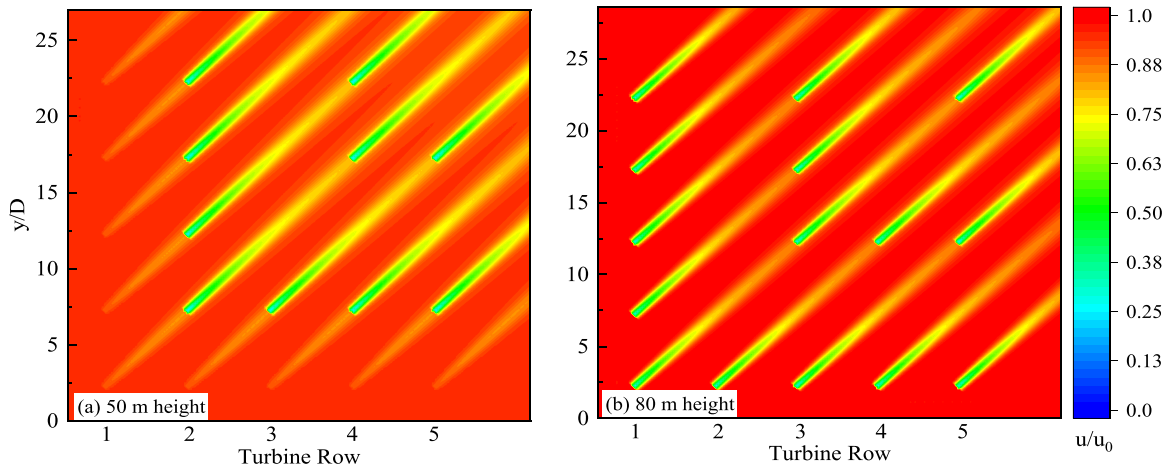


Figure 3: Normalized wind speed distribution at different heights (50, 80 m) after optimization.

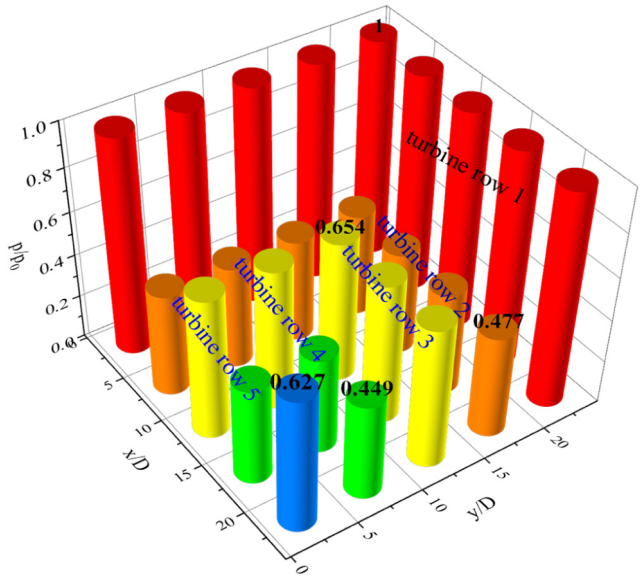


Figure 4: Normalized power generation of each turbine.

3.4 Case C3—Optimization of Layout (Position) at Uniform Height

In this scenario, with a fixed hub height of 80 m, the study investigates the layout optimization of turbines under a southwesterly inflow (225° meteorological direction; 45° downstream heading). Figs. 5 and 6 illustrate the normalized wind speed distribution and normalized power distribution at the hub height (80 m, *x*-*y* cross-section), respectively. The relevant conclusions are summarized as follows:

(a) For C3, the optimized turbine coordinates form a staggered layout that reduces wake overlap. Using the 80 m single-turbine reference power in Table 2, the minimum normalized turbine power is 260.41/345.10 = 75.46%. Moreover, 23 of the 25 turbines (92%) achieve normalized power outputs of at least 90%. These turbine-level values are consistent with the C3 total farm power of 8285.81 kW.

(b) Compared with the baseline case C1 at 80 m, the optimized C3 layout substantially improves downstream turbine performance. The minimum turbine power increases from 144.63 to 260.41 kW, and the total farm power increases from 5594.37 to 8285.81 kW. In normalized terms, the increase is from 16.21 to 24.01, corresponding to a 48.11% improvement relative to C1-80. If the lower 50 m aligned baseline is used as the reference, the increase is from 13.79 to 24.01, corresponding to 74.07%.

(c) The layout-only case C3 is also compared with the hub-height-only case C2. The normalized total power is 24.01 for C3 and 17.58 for C2. Their cost-per-normalized-power indicator values are 0.811 and 1.01, respectively. Thus, C3 produces more power and a lower indicator value than C2 under the present fixed turbine number, single inflow direction, and simplified cost formulation.

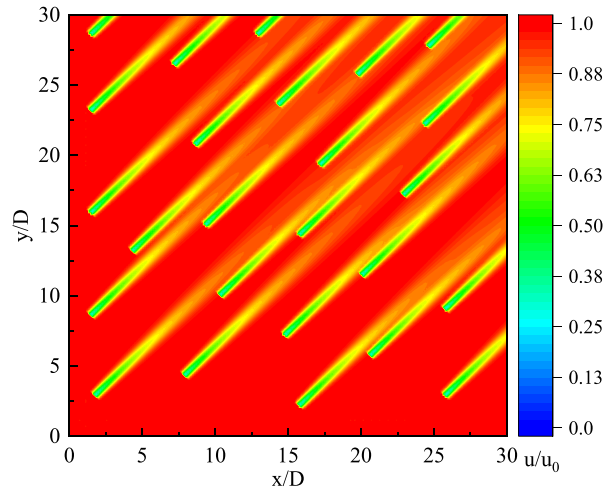


Figure 5: Normalized wind speed distribution at the hub height after optimization.

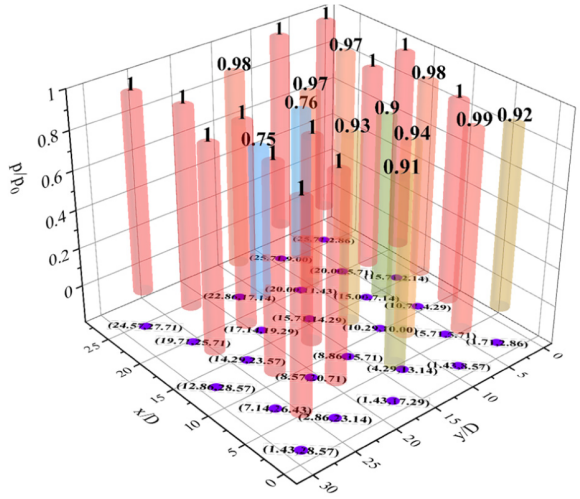


Figure 6: Normalized power distribution of each turbine after optimization (purple circles: turbine locations).

Table 2: Comparison of the results of each case using the cost-per-normalized-power indicator as the optimization objective.

Cases	Case-C1 (50 m)	Case-C1 (80 m)	Case-C2	Case-C3	Case-C4
Maximum Power (kW)	292.44	345.10	345.10	345.10	345.10
Mean Power (kW)	190.40	223.77	242.65	330.70	331.55
Minimum Power (kW)	124.47	144.63	154.80	260.41	261.02
Total Power (kW)	4759.91	5594.37	6066.15	8285.81	8288.81
Maximum Height (m)	50	80	80	80	80
Cost (USD)	15.93	19.48	17.75	19.48	19.48
Cost-per-Normalized-Power Indicator	1.16	1.20	1.01	0.81	0.81

3.5 Case C4—Simultaneous Optimization of Layout and Height

Case C4 simultaneously optimizes both turbine layout and hub height. Figs. 7 and 8 illustrate the normalized wind-speed distribution and normalized turbine power for the optimized solution. For the present two-height design space, the optimal hub-height assignment converges to 80 m for all turbines, so the C4 result is very close to the C3 layout-only solution. The minimum turbine power is 261.02 kW, and the total power and cost-per-normalized-power indicator are 8288.81 kW and 0.81, respectively, compared with 8285.81 kW and 0.81 for C3. This result supports the conclusion that, under the single prevailing wind direction and the two available hub heights considered here, turbine placement is the dominant control variable.

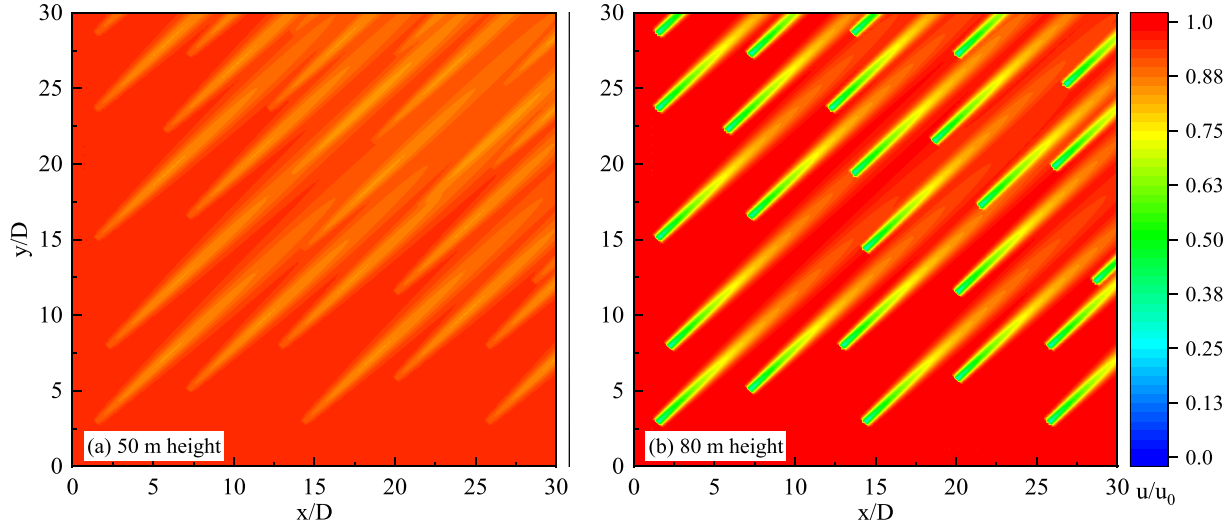


Figure 7: Normalized wind speed distribution at different heights (50, 80 m) after optimization.

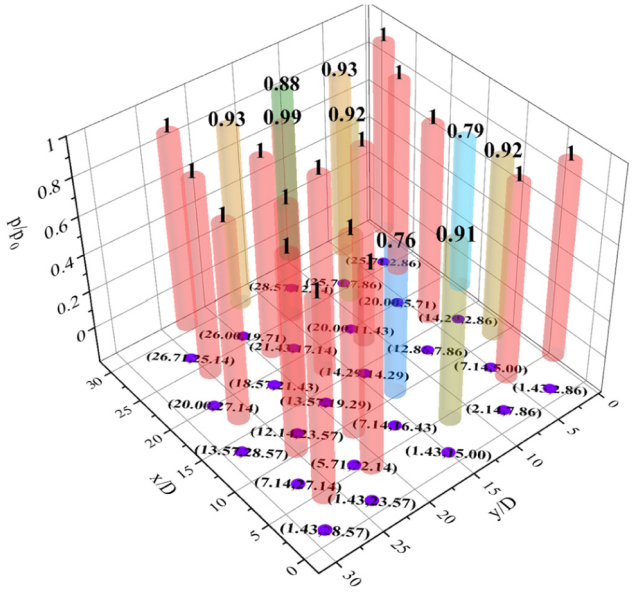


Figure 8: Normalized power distribution of each turbine after optimization (purple circles: turbine locations).

3.6 Discussion

Table 2 compares the computational results for all cases using the corrected cost-per-normalized-power indicator. The results show that C3 and C4 produce the highest total power outputs, 8285.81 and 8288.81 kW, respectively. The corresponding cost-per-normalized-power indicator values are both approximately 0.81, whereas C1-50, C1-80, and C2 have higher values of 1.16, 1.20, and 1.01, respectively. The identical cost values of 19.48 for C1-80, C3, and C4 arise because all three cases contain 25 turbines at 80 m and the simplified cost model in Eq. (5) has no layout-dependent term. Thus, layout optimization reduces the wake-loss penalty more effectively than height-only optimization for the present controlled wind direction. The conclusion is based on a single best GA run from the reported settings; because GA algorithms are stochastic, repeated-run statistics and convergence histories should be included in future extended studies to quantify optimization robustness.

3.7 Scope, Limitations, and Reproducibility Considerations

The present optimization is designed as a controlled comparison rather than a complete wind-farm design study. First, only one southwesterly inflow condition (225° meteorological direction; 45° downstream heading) is considered; a realistic wind rose with multiple directions and frequency weights may change the preferred layout and may increase the value of vertical staggering. Second, hub-height selection is restricted to two discrete options, 50 and 80 m, so the conclusion that height optimization has a smaller effect than layout optimization is specific to this limited height set. Third, the cost model is a simplified proxy based on turbine number and hub-height correction; it does not include cabling, foundations, installation vessels, operation and maintenance, terrain/seabed constraints, or grid-connection costs. Fourth, the reported GA solution corresponds to the best run obtained with the stated parameters. Future work should include repeated GA runs, convergence curves, and multi-direction wind roses to assess robustness and practical generality.

4 Conclusions and Future Remarks

This study develops an integrated wind farm layout optimization framework by coupling a previously validated 3DESG wake model with a GA method. The 3DESG wake model is reused from earlier work, while the present contribution is the optimization coupling, reproducible GA setup, and systematic comparison of fixed, height-only, layout-only, and coupled layout-height cases under a southwesterly inflow (225° meteorological direction; 45° downstream heading).

(1) Increasing the aligned baseline hub height from 50 to 80 m alleviates wake interference and increases total power from 4759.91 to 5594.37 kW. For the aligned layout, hub-height optimization further increases total power to 6066.15 kW and reduces the cost-per-normalized-power indicator from 1.20 for C1-80 to 1.01 for C2.

(2) Turbine arrangement exerts the dominant influence on wake mitigation in the controlled southwesterly-inflow case (225° meteorological direction; 45° downstream heading). Relative to the 80 m aligned baseline, layout optimization increases normalized total power from 16.21 to 24.01, corresponding to a 48.11% improvement, and reduces the cost-per-normalized-power indicator from 1.20 to 0.81. Relative to the 50 m aligned baseline, the corresponding normalized-power improvement is 74.07%.

(3) Layout-only optimization (C3) and simultaneous layout-height optimization (C4) produce nearly identical outcomes because the C4 search selects 80 m for all turbines in the present two-height design space. C3 and C4 achieve total powers of 8285.81 and 8288.81 kW, respectively, with cost-per-normalized-power indicator values of approximately 0.81. Therefore, the finding that layout

optimization dominates hub-height optimization should be understood within the assumptions of a fixed turbine number, a single wind direction, two discrete hub heights, and a simplified cost model.

The proposed 3DESG-GA framework provides an efficient controlled-analysis tool for WFLO. Future work will extend the method to multidirectional wind roses, broader hub-height ranges, higher-fidelity economic models, repeated GA runs with convergence statistics, and full reporting of the optimized turbine coordinates and hub-height assignments.

Acknowledgement: Not applicable.

Funding Statement: This work was supported by the National Natural Science Foundation of China (Grant No. 52178450), the Hubei Provincial Natural Science Foundation of China (2024AFB971), Wenzhou Applied Basic Research (Basic Research) Project (GK20250036), a University-Level Scientific Research Project of Wenzhou University of Technology (ky202519), and a Project Supported by Scientific Research Fund of Zhejiang Provincial Education Department (Y202559107).

Author Contributions: Lihua Mi: Conceptualization, Funding acquisition, Methodology, Software, Validation, Writing—original draft, Writing—review & editing. Xin Zhang: Resources, Software, Validation. Fei Zhang: Conceptualization, Supervision, Writing—review & editing. Hui Chen: Conceptualization, Project administration, Supervision, Validation. Pinhan Zhou: Resources, Software, Supervision, Validation. Qinghui Lai: Methodology, Software. All authors reviewed and approved the final version of the manuscript.

Availability of Data and Materials: The code used for the GA-based optimization and the numerical data supporting the tables are available from the corresponding author upon reasonable request.

Ethics Approval: Not applicable.

Conflicts of Interest: The authors declare no conflicts of interest.

References

1. Veers P, Dykes K, Lantz E, Barth S, Bottasso CL, Carlson O, et al. Grand challenges in the science of wind energy. Science. 2019;366(6464):eaau2027. doi:10.1126/science.aau2027.
2. Lundquist JK, DuVivier KK, Kaffine D, Tomaszewski JM. Costs and consequences of wind turbine wake effects arising from uncoordinated wind energy development. Nat Energy. 2019;4(1):26–34. doi:10.1038/s41560-018-0281-2.
3. Stanley APJ, Roberts O, King J, Bay CJ. Objective and algorithm considerations when optimizing the number and placement of turbines in a wind power plant. Wind Energ Sci. 2021;6(5):1143–67. doi:10.5194/wes-6-1143-2021.
4. Chen K, Song MX, Zhang X, Wang SF. Wind turbine layout optimization with multiple hub height wind turbines using greedy algorithm. Renew Energy. 2016;96:676–86. doi:10.1016/j.renene.2016.05.018.
5. Masoudi SM, Baneshi M. Layout optimization of a wind farm considering grids of various resolutions, wake effect, and realistic wind speed and wind direction data: a techno-economic assessment. Energy. 2022;244:123188. doi:10.1016/j.energy.2022.123188.
6. Ma Z, Zeng P, Lei L. Analysis of the coupled aeroelastic wake behavior of wind turbine. J Fluids Struct. 2019;84:466–84. doi:10.1016/j.jfluidstructs.2018.09.001.
7. Li T, Liu Z, Wang H, Bian W, Yang Q. Large eddy simulation for the effects of ground roughness and atmospheric stratification on the wake characteristics of wind turbines mounted on complex terrains. Energy Convers Manage. 2022;268:115977. doi:10.1016/j.enconman.2022.115977.
8. Cai Y, Zhao H, Li X, Liu Y. Effects of yawed inflow and blade-tower interaction on the aerodynamic and wake characteristics of a horizontal-axis wind turbine. Energy. 2023;264:126246. doi:10.1016/j.energy.2022.126246.
9. Ye M, Chen HC, Koop A. High-fidelity CFD simulations for the wake characteristics of the NTNU BT1 wind turbine. Energy. 2023;265:126285. doi:10.1016/j.energy.2022.126285.

10. Jia R, Ge M, Zhang Z, Li X, Du B. A numerical simulation framework for wakes downstream of large wind farms based on equivalent roughness model. Energy. 2024;307:132600. doi:10.1016/j.energy.2024.132600.
11. Tian L, Song Y, Wang Z, Zhao N, Zhu C, Lu X. Predictive capability of an improved AD/RANS method for multiple wind turbines and wind farm wakes. Energy. 2024;297:131207. doi:10.1016/j.energy.2024.131207.
12. Lee J, Kim DR, Lee KS. Optimum hub height of a wind turbine for maximizing annual net profit. Energy Convers Manage. 2015;100:90–6. doi:10.1016/j.enconman.2015.04.059.
13. Vasel-Be-Hagh A, Archer CL. Wind farm hub height optimization. Appl Energy. 2017;195:905–21. doi:10.1016/j.apenergy.2017.03.089.
14. Abdulrahman M, Wood D. Investigating the power-COE trade-off for wind farm layout optimization considering commercial turbine selection and hub height variation. Renew Energy. 2017;102:267–78. doi:10.1016/j.renene.2016.10.038.
15. Chen Y, Li H, Jin K, Song Q. Wind farm layout optimization using genetic algorithm with different hub height wind turbines. Energy Convers Manage. 2013;70:56–65. doi:10.1016/j.enconman.2013.02.007.
16. Yang Q, Hu J, Law SS. Optimization of wind farm layout with modified genetic algorithm based on Boolean code. J Wind Eng Ind Aerodyn. 2018;181:61–8. doi:10.1016/j.jweia.2018.07.019.
17. Liu Z, Fan S, Wang Y, Peng J. Genetic-algorithm-based layout optimization of an offshore wind farm under real seabed terrain encountering an engineering cost model. Energy Convers Manage. 2021;245:114610. doi:10.1016/j.enconman.2021.114610.
18. Bai F, Ju X, Wang S, Zhou W, Liu F. Wind farm layout optimization using adaptive evolutionary algorithm with Monte Carlo Tree Search reinforcement learning. Energy Convers Manage. 2022;252:115047. doi:10.1016/j.enconman.2021.115047.
19. Gao X, Yang H, Lu L. Optimization of wind turbine layout position in a wind farm using a newly-developed two-dimensional wake model. Appl Energy. 2016;174:192–200. doi:10.1016/j.apenergy.2016.04.098.
20. Sun H, Yang H. Wind farm layout and hub height optimization with a novel wake model. Appl Energy. 2023;348:121554. doi:10.1016/j.apenergy.2023.121554.
21. Song M, Chen K, Wang J. Three-dimensional wind turbine positioning using Gaussian particle swarm optimization with differential evolution. J Wind Eng Ind Aerodyn. 2018;172:317–24. doi:10.1016/j.jweia.2017.10.032.
22. MirHassani SA, Yarahmadi A. Wind farm layout optimization under uncertainty. Renew Energy. 2017;107:288–97. doi:10.1016/j.renene.2017.01.063.
23. Wen Y, Song M, Wang J. Wind farm layout optimization with uncertain wind condition. Energy Convers Manage. 2022;256:115347. doi:10.1016/j.enconman.2022.115347.
24. Mi L, Han Y, Li B, Chen H, Zhou P, Cai CS. An advanced analytical model for wind-turbine wakes based on an elliptic super-Gaussian function and adaptive parameters selection strategy. Phys Fluids. 2025;37(11):117136. doi:10.1063/5.0294148.
25. He R, Yang H, Sun H, Gao X. A novel three-dimensional wake model based on anisotropic Gaussian distribution for wind turbine wakes. Appl Energy. 2021;296:117059. doi:10.1016/j.apenergy.2021.117059.
26. Blondel F, Cathelain M. An alternative form of the super-Gaussian wind turbine wake model. Wind Energ Sci. 2020;5(3):1225–36. doi:10.5194/wes-5-1225-2020.
27. Lantz E, Roberts O, Nunemaker J, DeMeo E, Dykes K, Scott G. Increasing wind turbine tower heights: opportunities and challenges. Golden, CO, USA: National Renewable Energy Laboratory (NREL); 2019. Report No.: NREL/TP-5000-73629.